Sustainable Groundwater Decisions: Hydro-Economic Model Applications to Irrigation in Contrasting Environmental Conditions

Preprint Statement: This is a non-peer-reviewed preprint submitted to EarthArXiv.

The manuscript has not been peer-reviewed or formally published. Subsequent versions may differ slightly. The author retains the right to submit this manuscript to a peer-reviewed journal in the future.

Boyao Tian ¹ *

Andrea Brookfield ¹

Margaret Insley ²

David Rudolph ¹

¹Department of Earth and Environmental Sciences, University of Waterloo, 200 University Avenue West, Waterloo, ON, Canada, N2L 3G1.

²Department of Economics, University of Waterloo, 200 University Avenue West, Waterloo, ON, Canada, N2L 3G1.

^{1*} Corresponding Author: boyao.tian@uwaterloo.ca

Abstract

Groundwater is important for global agriculture but increasing populations and rising food demand are placing significant pressure on its sustainable use for irrigation. Effective, financially viable irrigation management strategies are urgently needed. This study applies a farm-level hydro-economic model to two contrasting sites: the High Plains Aquifer (HPA), a deep, overexploited, unconfined aquifer where overlying regions are almost entirely reliant on groundwater for irrigation; and the Saskatchewan River Basin (SRB), a relatively undepleted basin where overlying regions use both groundwater and surface water for irrigation. The model estimates groundwater availability and long-term land values while accounting for climate change impacts on crop production and irrigation practices. Using Conditional Value-at-Risk to assess economic risks, it offers robust recommendations for sustainable groundwater use. Results demonstrate distinct irrigation strategies: the HPA site faces greater potential economic and environmental impacts and requires increased irrigation to maintain productivity in the future; the SRB site experiences moderate impacts with little change needed to adapt to future climate scenarios. This divergence highlights how climate and water source variability shape trade-offs between economic returns and resource sustainability. This framework provides practical guidance for tailoring irrigation policies to regional conditions while managing risk under uncertain futures.

Keywords: Groundwater Management; Integrated Hydrologic Models; Risk Assessment Tool; Conditional Value-at-Risk; Analytical Models; Climate Change; Agricultural Water Management

1 Introduction

Groundwater is the largest accessible source of freshwater, supporting both ecosystems and human activities (Griebler and Avramov, 2015; Rohde et al., 2017; Mishra, 2023). It plays a particularly critical role in agriculture, where increasing population and food demands are placing unprecedented stress on crop production and groundwater resources (Misra, 2014; Islam and Karim, 2019; Hemathilake and Gunathilake, 2022). Regions such as North China Plain, High Plains Aquifer in the U.S., Guarani Aquifer in South America, known for their significant crop production, face severe irrigation water scarcity, threatening long-term sustainability (Foster et al., 2009; Cotterman et al., 2018; Yang et al., 2022). This highlights the urgent need for sustainable groundwater management strategies to mitigate stress, maintain resource viability, and balance economic outcomes.

Integrated hydro-economic models offer a valuable approach to simultaneously assess physical (e.g., geology, hydrogeology, climate, water use, land-use) and economic (e.g.,crop prices, capital costs) implications of agricultural land management, using optimization techniques and agent-based frameworks (Harou et al., 2009; Esteve et al., 2015; Ma et al., 2022; Ortiz-Partida et al., 2023; Lin et al., 2024; Yao et al., 2024). This paper builds on and applies a hydro-economic irrigation model that dynamically links groundwater availability with economic outcomes to support farm-level irrigation decision-making (Tian et al., 2025). The model's hydrologic component includes precipitation, evapotranspiration, groundwater availability and extraction, while the economic component estimates crop prices, irrigation costs, annual cash flows and long-term land values. Additionally, Conditional Value-at-Risk (CVaR) is utilized to evaluate potential economic risks associated with irrigation. This work extends the model through site-specific applications to evaluate sustainable agricultural water management under changing environmental conditions.

Climate change significantly impacts water resources, energy use, agriculture and other

socio-economic factors; and may result in increased precipitation in humid regions, prolonged droughts in arid areas, and more frequent extreme weather events (Fowler and Hennessy, 1995; Lambert et al., 2008; Zhang et al., 2022). Crop production is directly influenced by changes in temperature and precipitation, affecting evapotranspiration, soil moisture, and growing seasons (White et al., 2011; Cotterman et al., 2018; Ortiz-Bobea et al., 2021). This study applies RCP-based (Representative Concentration Pathway; Van Vuuren et al. (2011)) projections of precipitation and temperature to parameterize the yield model and assess their influence on land value and economic risk, thereby linking climate-driven changes in crop water demand and irrigation sustainability.

The main objective of this work is to advance and apply an integrated model for sustainable agricultural water management and informed irrigation decision-making under changing environmental conditions. Specifically, the study quantifies how alternative irrigation strategies and farmer's decisions influence both the expected land value and the associated risk, measured using the Conditional Value-at-Risk (CVaR) metric. These metrics reflect the key economic considerations of farmers and are central to evaluating the trade-offs between profitability and risk under water limitations. The irrigation strategies and farmer's decisions analyzed represent a reasonable range of options that farmers might realistically consider, and their performance is examined under differing regulatory constraints to assess how policy and water availability influence outcomes. To achieve this, the study: (1) incorporates climate factors to assess future impacts on crop production and irrigation practices; (2) applies the integrated model to two study sites with differing environmental conditions; and (3) demonstrates the utility of hydro-economic modelling for informing sustainable irrigation practices. By linking climate impacts, economic outcomes, and groundwater constraints, this work provides a practical and policy-relevant tool to support region-specific irrigation strategies.

2 Study Site

The hydro-economic model is applied to two farm sites in the High Plains Aquifer (HPA) in Kansas, U.S. and the Saskatchewan River Basin (SRB) in the Canadian Prairies. The HPA is a widely recognized example of groundwater overexploitation, primarily due to intensive irrigation, highlighting the urgent need for sustainable groundwater management to balance economic benefits with long-term resource conservation (Scanlon et al., 2012; Cotterman et al., 2018). The SRB has relatively abundant water resources but is facing rapid environmental change and water rights challenges (Gober and Wheater, 2014).

2.1 High Plains Aquifer

The High Plains Aquifer (HPA) spans ~450,658 km² underlies portions of eight U.S. states and supplies ~30% of the nation's groundwater for irrigation, making it one of the most critical regions for crop production (Steward et al., 2013; Sahoo et al., 2017; Ajaz et al., 2020). However, extensive over-extraction and low recharge have led to significant declines in water levels, particularly in the south and central HPA, posing serious challenges to the sustainability of long-term crop production (Chen et al., 2016; Smidt et al., 2016). Groundwater serves as a buffer against drought; however, due to aquifer depletion, crops have a diminishing capacity to withstand drought conditions (Hund et al., 2018; Mieno et al., 2024). The HPA has a semi-arid climate, where climate change is projected to bring higher temperatures and reduced precipitation; increasing drought frequency and severity will further exacerbate these challenges, negatively affecting crop yields and overall agricultural productivity (Cotterman et al., 2018; Ji and Senay, 2023; Mieno et al., 2024). In Kansas, groundwater rights are linked to land rights and governed by prior appropriation, with water rights limits (total volume and rate), as well as water use measurement and reporting requirements (Peck, 2015; Edwards, 2016; Kansas Water Appropriation Act, 2022).

For this study, an irrigation well in Haskell County, southwest Kansas was chosen (Figure 1). This well pumps groundwater from the HPA, which has an estimated hydraulic conductivity of $\sim 3 \times 10^{-4}$ m/s, specific yield of 0.175, and initial saturated aquifer thickness of ~ 60 m (Cederstrand and Becker, 1998; USGS, 2023a,b). Pumping volumes, constrained by water rights, were obtained from the Water Information Management and Analysis System (WIMAS) (KGS, 2025). Based on United States Department of Agriculture (USDA) data, corn is selected as the main crop of this site (USDA, 2017).

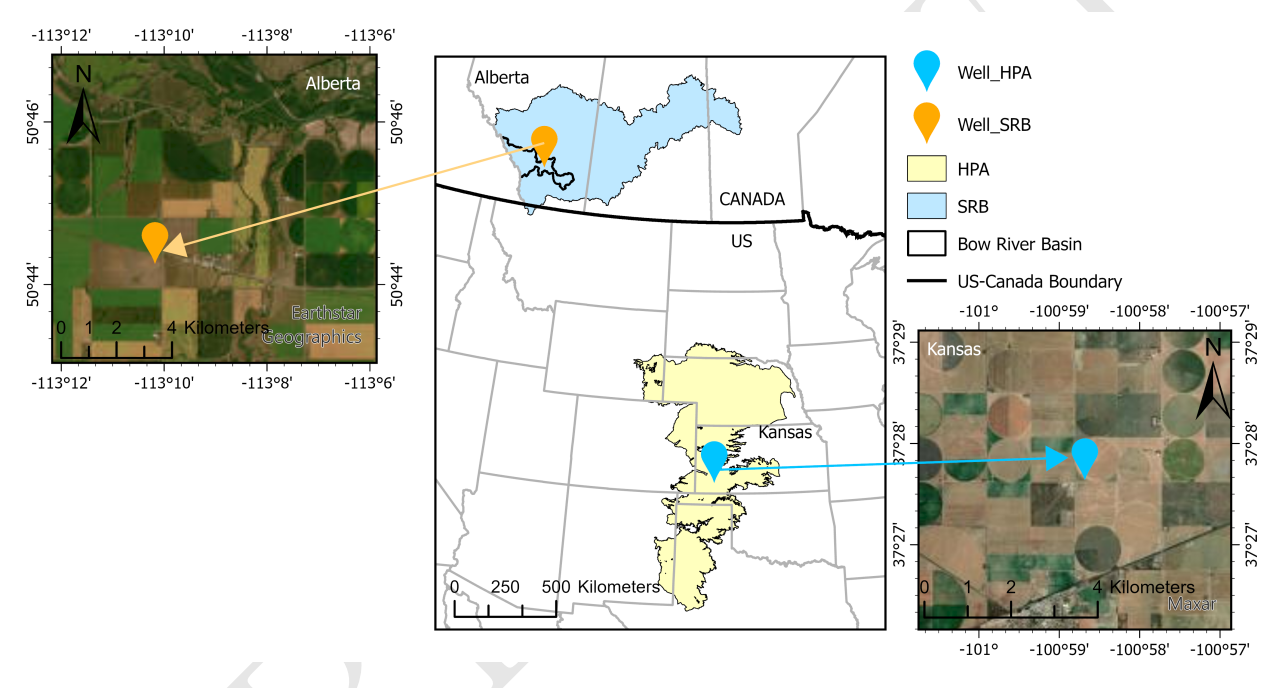


Figure 1: Locations of target wells in the HPA and the SRB; data for the HPA is from Qi (2010), and data for the SRB is from AFCC (2013).

2.2 Saskatchewan River Basin

The Saskatchewan River Basin (SRB) has a total drainage area of ~406,000 km², and underlies the southern Canadian Prairies, with 80% of its runoff derived from Rocky Mountain snowmelt (Pomeroy et al., 2005; Masud et al., 2015). The SRB supports 75% of Canada's irrigated agriculture, is a major food-producing region in Canada, and a globally significant

natural resource development site (Corkal et al., 2011; Gober and Wheater, 2014). Specifically, in the south SRB, irrigation accounts for over 90% of all consumptive water use and directly withdraws ~22% of the natural river flow (Bruneau, 2009; Corkal et al., 2011). Future water availability has significant uncertainty due to climate change; extreme weather events, such as droughts and increased snowmelt, may lead to instability in surface water supplies, resulting in increasing reliance on groundwater resources (Bates et al., 2008; Taylor et al., 2013; Scanlon et al., 2023).

For this study, an irrigation well located in Vulcan County, southern Alberta (Figure 1), was selected. This well pumps groundwater from the Buried Valleys Aquifer System (confined aquifer), with an estimated hydraulic conductivity of 10^{-4} m/s, a specific storage of 10^{-4} m⁻¹, and an initial aquifer thickness of ~35 m (Cummings et al., 2012; GIN, 2021). The data for this target well is from Alberta Water Well Information Database, and the pumping data used in this model is constrained by water license under Alberta's Water Act (Government of Alberta, 2020, 2023, 2024c). Based on Government of Alberta (2024b), barley is selected as the main crop type in Vulcan County.

3 Methods

The integrated hydro-economic model includes precipitation, groundwater, crop yield, economic and risk assessment models. This section briefly outlines these model components (more detail available in Tian et al. (2025)). We simplified the hydrologic section to conceptual models representing unconfined (HPA case) and confined (SRB case) aquifers under a single-layer assumption (Figure 2). All equations in this section apply to both cases, and parameters are listed in Supplementary A.

(a) Conceptual Model: Unconfined Aquifer (b) Conceptual Model: Confined Aquifer Groundwater Groundwater Precipitation Precipitation Residual Drawdown Residual Drawdown Drawdown Pressure Head New New Aquifer Hydraulic Hydraulic Saturated Head Aquifer Thickness Head Elevation Head Unconfined Aquifer

Figure 2: Conceptual models of (a) unconfined aquifer and (b) confined aquifer (Tian et al., 2025).

3.1 Precipitation Model

Precipitation is simulated using a simple first-order Markov chain exponential model based on Richardson (1981), and rainfall analysis is conducted using an exponential distribution. Detailed steps can be found in Tian et al. (2025). Site specific models are based on weather data at Sublette 7WSW weather station for the HPA (High Plains Regional Climate Center, 2024) and Mossleigh AGCM weather station for the SRB (Alberta Climate Information Service, 2024).

3.2 Groundwater Model

The groundwater model used here is adapted from Tian et al. (2025), which includes recharge, drawdown and recovery, and groundwater storage dynamics. Here, we only present the adjustments made to suit the specific conditions of the two study sites.

3.2.1 Groundwater Recharge

This model can be applied to shallow aquifers, where recharge occurs directly from precipitation and irrigation within the pumping period; as well as to deep aquifers, where recharge takes decades or even centuries to reach the aquifer. For the latter, a temporally variable rate can be assumed by model users. As the HPA is a deep aquifer, and based on previous studies, we applied a constant annual recharge rate of ~0.0228 m/year (Stanton, 2013). Since the target well in SRB is in Buried Valley Aquifer, which is a confined aquifer; the aquifer thickness remains constant despite pumping or recharge processes. The till aquitards that cover buried valleys limit recharge to Buried Valley Aquifer, therefore, this model simplified recharge as a constant rate of ~0.002 m/year (Cummings et al., 2012; GIN, 2021).

3.2.2 Groundwater Drawdown

Drawdown from the target well is calculated using Cooper and Jacob's method (Cooper Jr and Jacob, 1946), with corrections for unconfined aquifers, neighbouring wells, and well efficiency as described by Brookfield (2016). In the HPA case, all these factors are considered. Since the pumping wells in SRB are far apart from each other, the additional drawdown caused by pumping from neighboring wells was found to be insignificant and is therefore excluded from this model; so the additional drawdown for SRB is only from additional loss in hydraulic head due to well inefficiency.

3.3 Crop Yield Model

The yield function, modified by Martin et al. (2010) and Klocke (2011), is utilized in this paper, with details available in Tian et al. (2025). This function represents the nonlinear relationship between crop yield and evapotranspiration, capturing diminishing returns in

crop yield as water input increases. This yield model is updated to account for climate change impacts, as outlined in Section 3.6.

3.4 Economic Model

The economic model determines land values with crop prices and associated costs. The state variables at time t are stochastic precipitation $P_E(t)$, available water in the aquifer B(t), irrigation requirement $I_r(t)$, and stochastic price P(t). The irrigation fraction (β) , determined by farmers or regulators, is a control variable representing the percentage of water applied relative to the crop water demand (i.e., the amount of water required to achieve maximum yield). All functions are defined on an annual time scale.

3.4.1 Price Model

This study models crop prices using a Mean Reverting (MR) stochastic process, with the governing equations and discrete-time approximation detailed in Tian et al. (2025). We adopt a time step of 1/12 year to capture monthly dynamics. For the HPA site, monthly corn prices received by farmers (USDA, 2024) from January 2015 to May 2024 were deflated using the Consumer Price Index (U.S. Bureau of Labor Statistic, 2024). For the SRB site, we used similarly deflated monthly barley prices reported by Statistics Canada (2024). Parameters were estimated using ordinary least squares regression following Insley and Wirjanto (2010), with the resulting coefficients summarized in Supplementary A.

Since the growing season in the HPA ends in September, we use October corn prices to calculate land values; while for the SRB, with its May-August season, September barley prices are applied. The price simulation spans 150 years, and for operation years exceeding this horizon, the 150^{th} year price is used, as discounting minimizes the impact of long-term prices. Results from 10,000 Monte Carlo price simulations and Maximum Likelihood

Estimation for validation are provided in Supplementary B.

3.4.2 Cost Functions

The cost function is the same as presented in Tian et al. (2025), including pumping cost, yield-related cost, and fixed cost. It is notable that we use the distance for lifting water from subsurface to the ground surface (ΔH_{lift} [m]) to estimate energy usage, which determines the pumping cost for groundwater. However, in the SRB site, part of the irrigation comes from the Bow River, making it necessary to account for both the lifting distance of groundwater and friction loss (ΔH_{loss} [m]) of surface water during transport. Therefore, the energy usage of pumping is modified from Alam et al. (2023):

Energy Usage =
$$\begin{cases} \frac{Q_{gw}\Delta H_{lift}t_p\rho g}{3.6\times 10^6\eta_p}, & \text{HPA} \\ \frac{(Q_{gw}\Delta H_{lift} + Q_{sw}\Delta H_{loss})t_p\rho g}{3.6\times 10^6\eta_p}, & \text{SRB} \end{cases}$$
(1)

where Q_{gw} and Q_{sw} is the pumping rate from groundwater and surface water respectively; t_p is pumping days per year; ρ is water density [kg/m³]; g is gravity factor [m/s²]; η_p is pumping efficiency [-]. At our study site, the elevation of nearby surface water body is 981 m, which is higher than the target well (960.9 m), allowing water to be delivered by gravity. Therefore, for SRB, the friction loss is estimated as 4.5 m per 100 m for a 6-inch PVC pipe.

3.4.3 Irrigation Decisions

This paper also follows the hydro-economic framework, where the irrigation fraction (β) represents the farmer's irrigation decision, defined as the percentage of crop water demand required to achieve maximum yield. Regulatory constraints (pumping limits and extraction rules) and physical parameters are kept consistent with the previous case.

3.4.4 Expected Land Value

Annual cash flow and expected land value are calculated following the approach of Tian et al. (2025). Annual cash flow is determined by crop yield, crop price, and production costs. Expected land value is obtained as the present value of annual cash flows over time, and depends on the state variables $P_E(t)$, B(t), $I_r(t)$, and P(t), as well as the decision variable β .

3.5 Risk Assessment Model

This study uses Conditional Value-at-Risk (CVaR) for the risk assessment model. CVaR focuses on tail risks to capture rare but severe events, which is more effective compared to traditional risk measures such as simple standard deviation or Value-at-Risk (Rockafellar et al., 2000; Rockafellar and Uryasev, 2002; Filippi et al., 2020). CVaR has been widely applied in fields such as medicine, supply chain management, hazardous material transportation, and energy management, offering valuable insights for optimal decision-making (Xu et al., 2013; Faghih-Roohi et al., 2016; An et al., 2017; Filippi et al., 2020; Xuan et al., 2021). However, its application in groundwater management remains rare. Our hydro-economic risk model presents a novel approach by integrating CVaR with agricultural water management strategies, providing a more comprehensive framework for assessing economic risk in groundwater-dependent farming.

In this study, the 95% CVaR is defined over the distribution of expected land values, representing the average expected land value in the worst 5% of cases, rather than losses. Therefore, a larger CVaR indicates higher expected land values in the worst-performing (lower-tail) outcomes, reflecting reduced downside risk and greater economic resilience. This interpretation contrasts with the conventional loss-based definition, where a higher CVaR would represent greater risk. The 95% relative CVaR represents the deviation between

the average of the worst 5% of simulated land values and the overall expected land value, providing a measure of downside risk relative to the average outcome.

3.6 Climate Change

Climate impacts were considered using data derived from Representative Concentration Pathway (RCP) projections, which provide standardized greenhouse gas concentration pathways for climate modeling (Van Vuuren et al., 2011). Rather than running climate projections directly, this study uses pre-modeled outputs of temperature and precipitation changes under RCP4.5 and RCP8.5, incorporating percentage changes in precipitation and shifts in minimum and maximum temperature into the yield model. Climate factors for the 20-year horizon are based on 2010–2040 results, and long-term parameters are derived from 100-year simulations. Data for the HPA site were obtained from The Climate Explorer (2024) and for the SRB site from Climate Data (2024). These data were selected for their regional relevance and widespread use, ensuring consistent parameterization across both sites (Table 1). Users may adapt the model to other available datasets or scenarios as needed.

Table 1: Climate factors used for HPA and SRB. T=20 denotes a 20-year time scale, while T=TD refers to pumping continues until aquifer depletion.

	HPA				SRB			
Climate Scenario	RCP 4.5		RC	RCP 8.5 RCI		P 4.5	RCP 8.5	
Time Scale	T=20	T=TD	T=20	T=TD	T=20	T=TD	T=20	T=TD
Precipitation	-2.0%	-2.90%	-3.8%	-5.2%	+4.97%	+5.97%	+5.89%	+8.01%
Max Temp. (°C)	+1.5	+2.3	+1.5	+3.1	+1.5	+2.4	+1.6	+3.4
Min Temp. (°C)	+1.4	+2.1	+1.5	+2.9	+1.5	+2.5	+1.7	+3.6

Under climate change scenarios, the impacts of precipitation on crop yield are captured using the following yield functions to estimate non-irrigated yield (rain-fed yield), modified from Martin et al. (2010) and Klocke (2011):

$$Y_n = b_{cc} Y_m \left[1 - \left(1 - \frac{P_E}{ET_p} \right)^{\frac{ET_p}{P_E}} \right]$$
 (2)

where Y_n is the non-irrigated yield [bu/ac]; Y_m is the maximum yield [bu/ac], P_E is the effective precipitation [mm/yr]; ET_p is the potential evapotranspiration required to achieve the maximum yield [mm/yr]. b_{cc} is a yield factor used to scale non-irrigated yields under original conditions to match site-specific yield data. Then, this Y_n is applied to the yield function modified from Martin et al. (2010) and Klocke (2011) to estimate actual yield under different scenarios, where Y_a is the estimated yield [bu/ac]; I_d is irrigation decision [m]; I_r is maximum irrigation requirement [m]; I_e is irrigation efficiency [-]:

$$Y_a = Y_n + (Y_m - Y_n) \left[1 - \left(1 - \frac{I_d}{I_r} \right)^{\frac{1}{I_e}} \right]$$
 (3)

4 Results

Simulations for the two study sites are conducted for T=20 years and T=TD (until aquifer depletion), focusing on irrigation fraction (the percentage of water applied relative to the amount needed to maximize yield), sustainable regulatory constraints (maximum pumping limits and extraction rules), groundwater-surface water ratios (SRB site only), and climate change impacts (Table 2; climate parameters in Table 1). Each scenario is analyzed using 10,000 Monte Carlo simulations and a 2% discount rate unless otherwise specified.

Table 2: List of variables tested across scenarios.

Symbol	Description	HPA	SRB
β	Irrigation Fraction [-]	[0.7, 1]	[0.7, 1]
$ar{I}$	Regulatory Pumping Limit [m ³ /day]	[2000, 5000]	[300, 1000]
μ	Sustainable Extraction Rule [-]	[0.2, 1]	[0.3, 1]
GW/SW	Groundwater-Surface Water Pumping Ratio [-]	_	[0, 1]

4.1 Irrigation Strategies

In this section, we evaluate six groups of irrigation strategies based on local conditions (Table 3): (A) no regulatory pumping limit (\bar{I}) with varying irrigation fractions (β); (B) constant regulatory pumping limits with varying irrigation fractions; (C) time-varying regulatory pumping limits with a fixed irrigation fraction (two-stage), following a large-to-small pattern; (D) time-varying regulatory pumping limits with a fixed irrigation fraction, following a small-to-large pattern. (E) time-varying irrigation fractions (two-stage) with a fixed pumping limit, following a large-to-small pattern; and (F) time-varying irrigation fractions with a fixed pumping limit, following a small-to-large pattern. The tested strategies reflect real-world irrigation practices and local regulatory constraints.

4.1.1 HPA Site

In the HPA case (Figure 3), land values initially increase with increased regulatory pumping limit. For T=20 years (Figure 3 a-c), land value peaks at \sim \$900k when $\beta=1$ under a limit of 3400 m³/day, while the corresponding CVaR is only \sim \$550k and relative CVaR is \sim 38%. The 95% CVaR in Figure 3b represents the average expected land value within the worst 5% of simulated outcomes, reflecting potential economic performance under unfavorable conditions such as droughts (from the stochastic precipitation model) or low crop prices (from the stochastic price model). In other words, while the expected land value reflects the average return, the CVaR quantifies the downside risk where the level of financial performance a farmer might experience when conditions are particularly adverse. The 95% relative CVaR in Figure 3c represents the difference between the average of the worst 5% of land value outcomes and the overall expected land value across all simulations.

For $\beta = 0.8$, the peak occurs earlier at 3000 m³/day, because the lower irrigation fraction dominates actual water use and the regulatory limit no longer constrains pumping. However,

Table 3: Irrigation strategies for HPA and SRB sites.

	Irrigation	n Fraction (β)	Regulatory Pumping Limit (\bar{I})				
Group	HPA	and SRB	H	IPA	S	SRB	
	$t \le T/2$ $t > T/2$		$t \leq T/2$	t > T/2	$t \leq T/2$	t > T/2	
A1		1		_		_	
A2		0.9		_		_	
B1		1	[2000, 500	0] (step 200)	[300, 1000	0] (step 100)	
B2		0.9	[2000, 500	0] (step 200)	[300, 1000	0] (step 100)	
В3		0.8	[2000, 500	0] (step 200)		-	
C1		1	3900	3700	750	650	
C2		1	3800	3600	700	600	
C3		1	3500	3400		_	
C4		1	3400	3300		-	
D1		1	3700	3900	650	750	
D2		1	3600	3800	600	700	
D3		1	3400	3500		_	
D4		1	3300	3400		_	
E1	1	0.9	3	3400	ı	700	
E2	1	1 0.8		3400		700	
E3	0.95	0.85	3	3400	1	700	
E4	0.9	0.8	3	3400	1	700	
F1	0.9	1	3	3400	I	700	
F2	0.8	1	3	3400		700	
F3	0.85	0.95	3400		700		
F4	0.8	0.9	3	3400	ı	700	

the reduced irrigation drives CVaR down to \sim \$100k, an extremely low outcome compared to other scenarios that would be undesirable in practice. T=TD cases show similar patterns in Figure 3 d-f. An increase in the discount rate from 2% to 5% results in smaller range of land values because future income is discounted more heavily, reducing its present value (Figure 3 a, d). CVaR follows a trend similar in land values. The large variations in the relative CVaR figures (e.g., between 2400 and 2600 m³/day) correspond to the transition of land values from negative to positive.

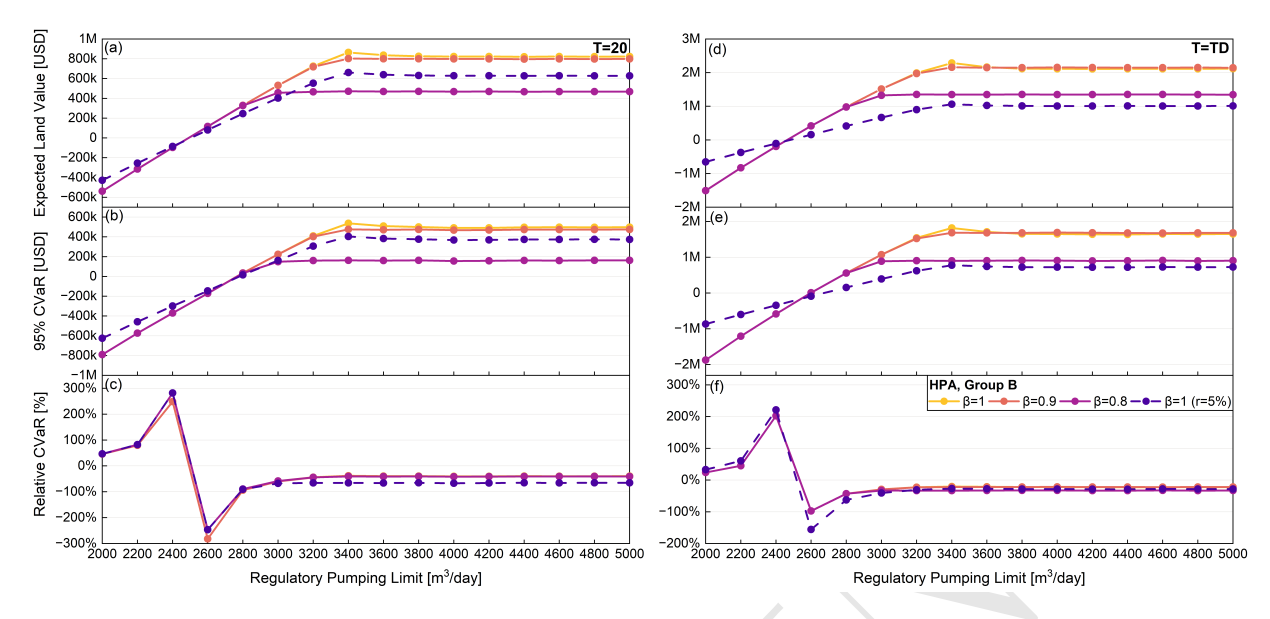


Figure 3: Expected land value, 95% CVaR and 95% relative CVaR for irrigation strategy group B at the HPA site. (a-c) T=20; (d-f) T=TD.

The farmer's decision variable, irrigation fraction (β), was tested over the range 0.7–1.0. In the HPA case, higher irrigation fractions shorten the operational period from 339 to 255 years but increase land values, which peak at $\beta = 0.95$ (Figure 4a1). Notably, relative CVaR declines sharply and stabilizes beyond $\beta = 0.85$, suggesting it may serve as a critical indicator for guiding irrigation fraction decisions.

Figure 5 shows the outcomes of different irrigation strategies for the HPA outlined in Table 3. In addition to CVaR, we include standard deviation to capture overall variability, providing a complementary measure to CVaR. Overall, expected land value and 95% CVaR display a linear relationship. Under T=20, group E and F have the lowest values, but strategy E1 and F1 perform relatively better, as applying more than 90% of crop water demand balances pumping costs with production benefits. Front-loaded strategies (group C) generally achieve higher land values, as discounting favors near-term returns. Strategies C1, C2 align with the crop water demand (~3700 m³/day), while strategies C3 and C4 set pumping limits closer to the point of maximum land value identified in Figure 3, corresponding to operational periods of ~85 and ~95 years, respectively. Although strategies C3 and C4 do

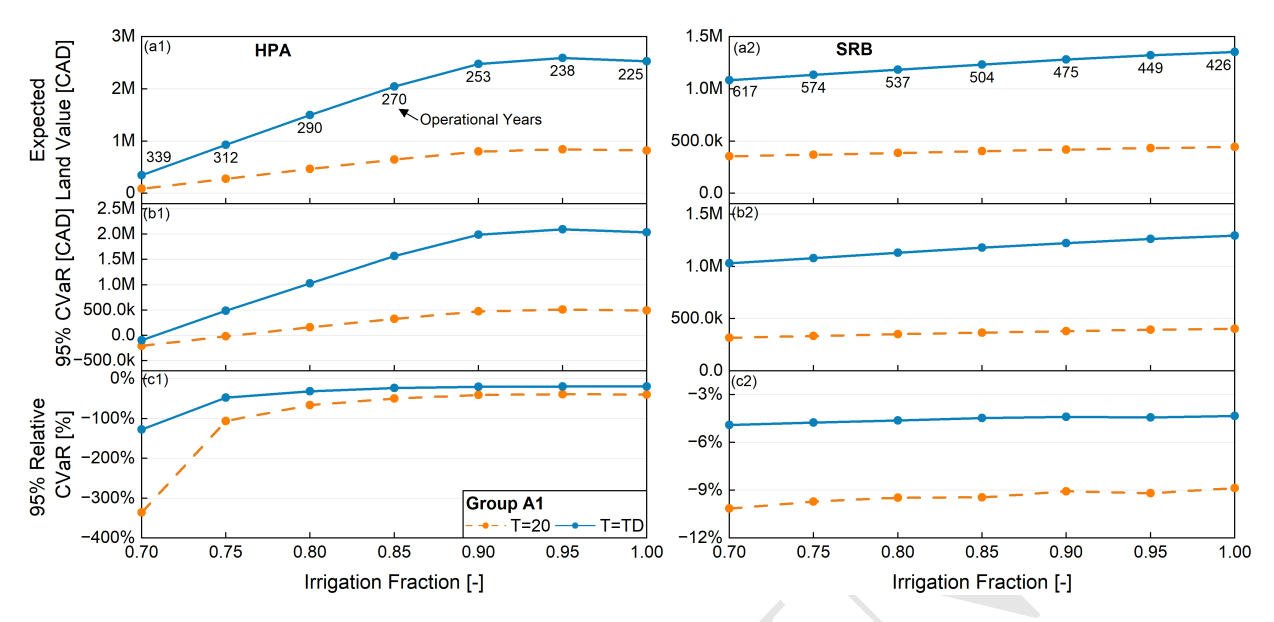


Figure 4: Expected land values and CVaR results for different irrigation fractions: (a1-c1) HPA farm site; (a2-c2) SRB farm site, with labels indicating the number of operational years for T=TD cases.

not fully meet water demand, they yield higher land values due to lower pumping costs and longer operational lifetimes. Differences among other nearby strategies are relatively small (within $\sim 10\%$ of land value).

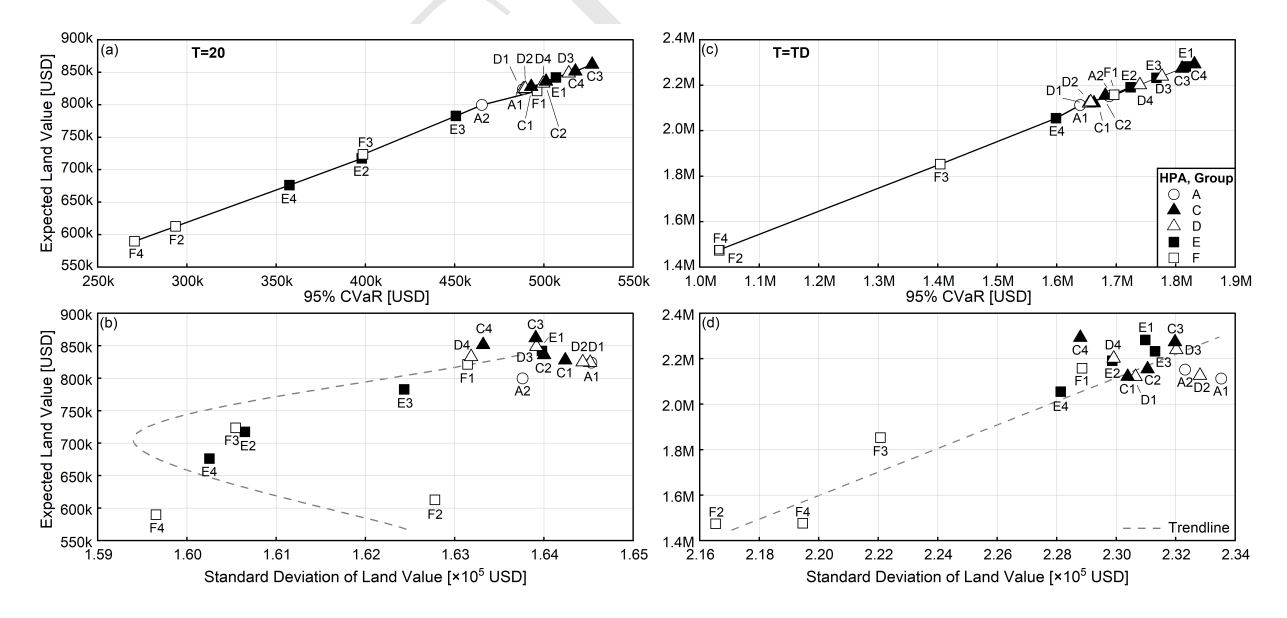


Figure 5: Relationships between expected land value and risk metrics: (a, c) 95% CVaR; (b, d) standard deviation, across irrigation strategies at the HPA site.

In Figure 5b and d, strategy A1 consistently shows the largest standard deviation, as it operates without any regulatory pumping limit, making irrigation demand highly sensitive to precipitation fluctuations. While many strategies yield comparable expected land values and similar CVaR results, their variability differs substantially. This demonstrates that standard deviation only measures the spread of outcomes, without indicating whether variability is beneficial or harmful. In practice, decision-makers are concerned with both downside risk (captured by CVaR) and overall volatility (captured by standard deviation), and together these metrics provide a more robust basis for irrigation decisions.

In addition to land value, annual cash flows are critical for farmers, allowing them to manage purchases and debt. Figure 6 presents annual cash flows and corresponding CVaR over time. Across both horizons, values generally increase in the early years and decline later due to discounting, with a pumping limit of 3400 m³/day generating the highest outcomes. Peak annual cash flows occur around years 6–7 for all pumping limits. For T=TD, pumping limit at 3000 m³/day results in consistently negative CVaR values that gradually approach zero. Under more relaxed pumping limits, CVaR is often negative in the first five years, peaks near year 10, and then declines toward zero. To further understand how water depth (WD) dynamics contribute to this pattern, we examined the relationship between cash flow and WD (Figure 7). The steepest derivatives occur around years 6–7, consistent with peak annual cash flows. This pattern is driven by the dynamics of the cone of depression (Figure 2). As pumping continues, the cone expands, and drawdown increases. Around years 6-7, the cone reaches a critical size where even small additional increases in drawdown release relatively large amounts of water with low pumping costs. This also reflects a critical window where crop yields remain strong, discounting has not yet substantially reduced returns, and groundwater extraction is more profitable.

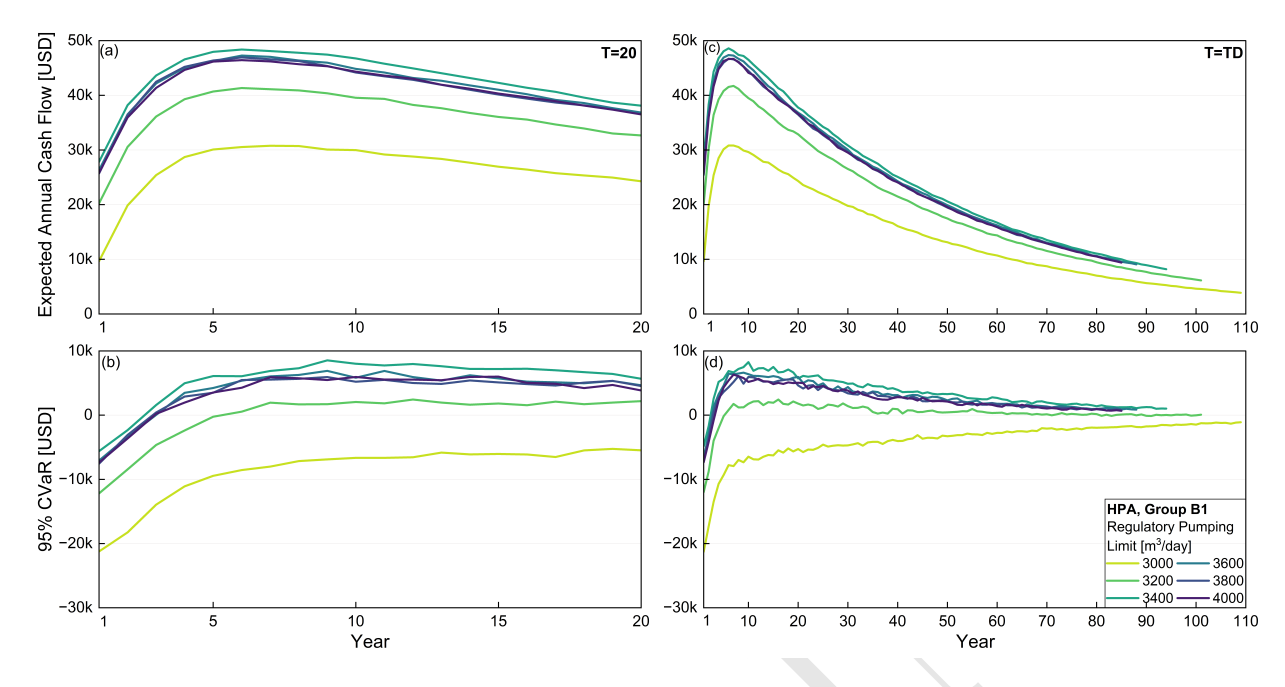


Figure 6: (a, c) Expected annual cash flow; (b, d) corresponding CVaR of strategy group B1 in the HPA site.

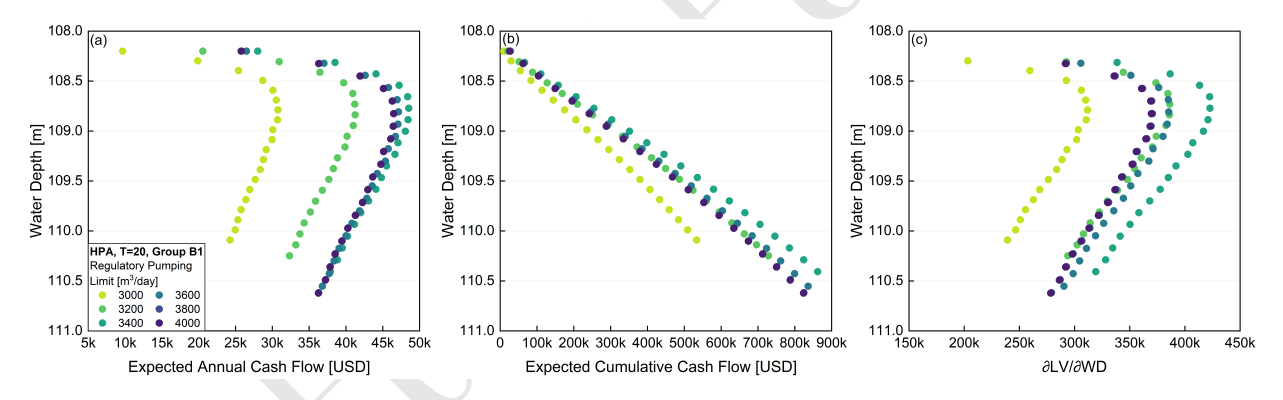


Figure 7: Relationships between (a) expected annual cash flow, (b) expected cumulative cash flow, (c) sensitivity of land value to water depth ($\partial LV/\partial WD$), and water depth for strategy B1 in the HPA site, T=20.

4.1.2 SRB Site

In the SRB simulations, the regulatory pumping limits represent the combined use of groundwater and surface water. A range of groundwater-surface water ratios was tested (Table 2, Figure 8), with a default setting of 67% groundwater and 33% surface water based

on local water allocation rules. Results indicate that higher groundwater use generally yields greater land values. This is primarily due to the relatively shallow aquifer, which reduces pumping costs; and the high delivery costs of transporting surface water to the target well, located far from the stream.

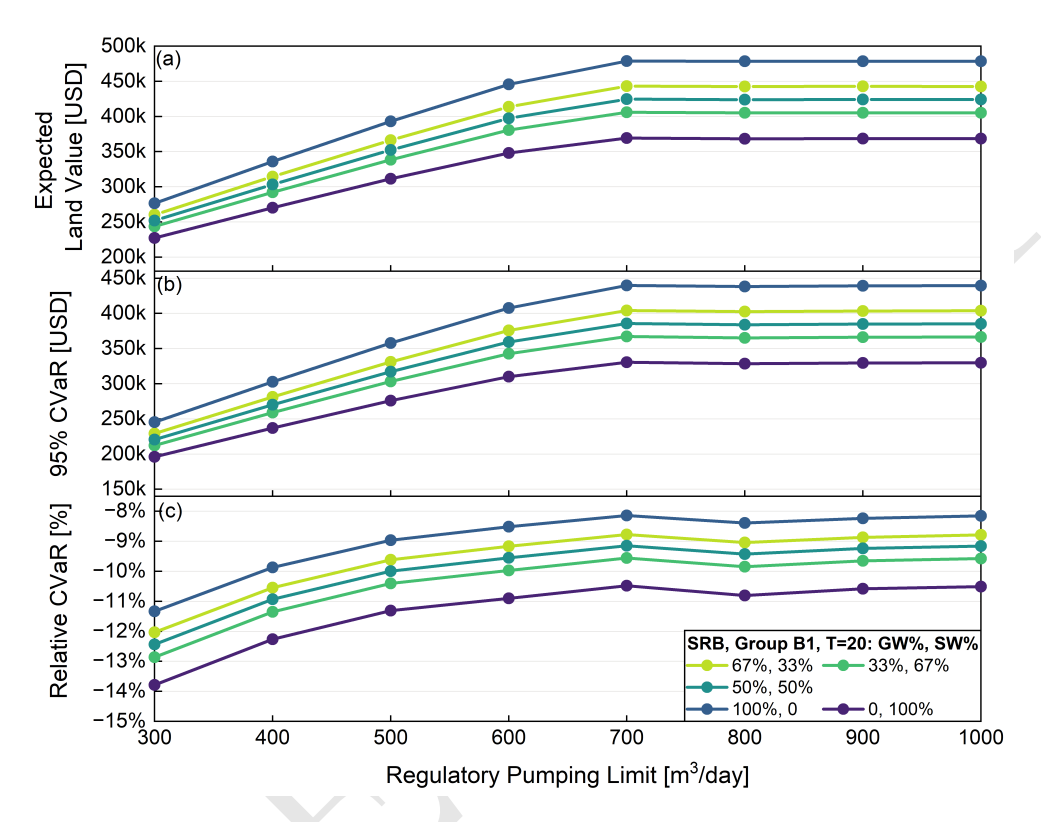


Figure 8: (a) Expected land values, (b) 95% CVaR and (c) relative CVaR for different pumping ratios in the SRB simulations.

Unlike the HPA site, the SRB site reaches its highest land values at a pumping limit of ~700 m³/day, which closely matches crop water demand. Therefore, the tested irrigation strategies are around this value (Table 3). Groups E and F still generate relatively low land values; however, in Figure 9c, strategy E1 produces the highest land value, with A1 close behind. In E1, allocating 90% of irrigation to the later half of the timescale reduces water use and pumping costs, while long-term discounting further lessens its impact. For T=20 years, front-loaded (C) and back-loaded (D) pumping limits result in similar outcomes because the SRB site relies on two water sources. However, for T=TD, greater early-year pumping yields

higher land values, as discounting reduces the weight of distant future returns.

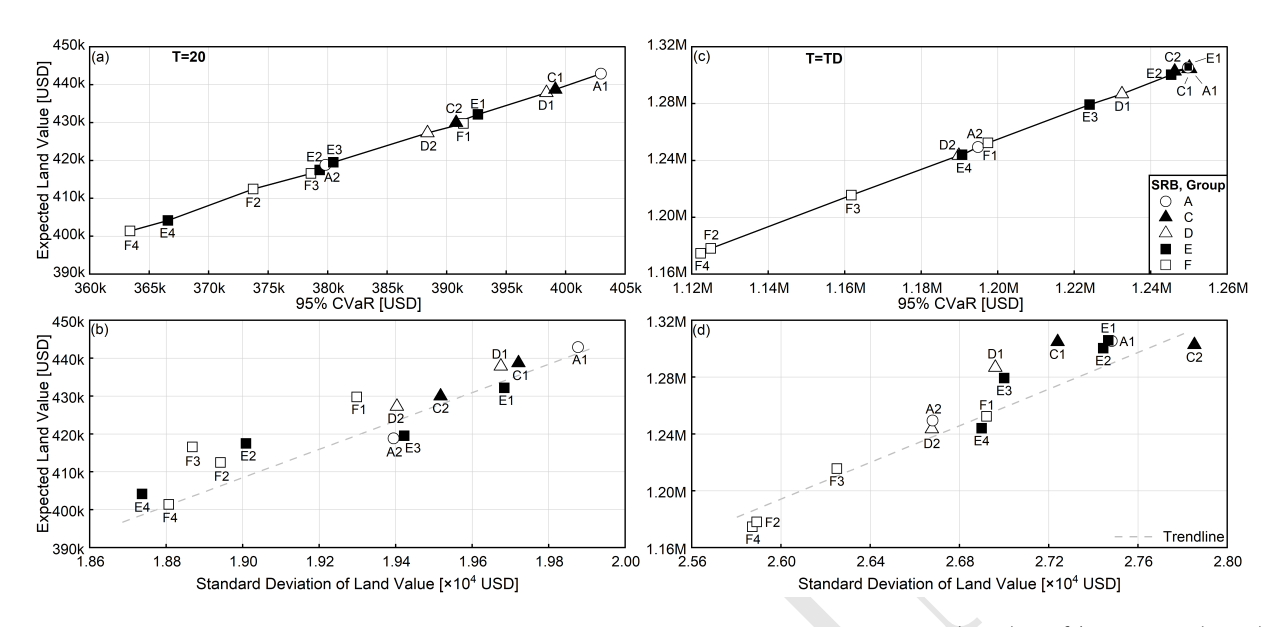


Figure 9: Relationships between expected land value and risk metrics: (a, c) 95% CVaR; (b, d) standard deviation, across irrigation strategies at the SRB site.

In Figure 9b and d, the standard deviation $(\times 10^4)$ is an order of magnitude lower than that of the HPA site $(\times 10^5)$, indicating reduced variability. Certain strategies (e.g., C1, C2, E1 in the TD case) exhibit similar land values but differ significantly in standard deviation, whereas others (e.g., A2, D2 in the 20-year case) show comparable risk but notable differences in land values. However, standard deviation is a limited risk metric because it captures both upside and downside variability, potentially overstating risk by treating favorable outcomes as equally undesirable as losses. By contrast, CVaR directly measures downside risk and focuses on the lower tail of the distribution, making it more informative for irrigation decisions where avoiding worst-case outcomes is critical.

At the SRB site, increasing irrigation fractions lead to higher land values (Figure 4 (a2-c2)). For the TD case, operational years range from 617 to 426, while CVaR only slightly lower than the expected land value (\sim 5%, Figure 4(c2)). This occurs because the long operational horizon (>400 years) amplifies discounting effects, minimizing variability. For the T=20 case, relative CVaR also remains very small (\sim 10%), indicating highly stable

conditions compared to other scenarios. The annual cash flow analysis, exhibiting similar trends to the HPA site, is presented in Supplementary C.

4.2 Sustainable Extraction Rule

This section evaluates one possible sustainable regulatory constraint: the sustainable extraction rule (μ) , defined as the allowable percentage of initial aquifer thickness (Table 2). This type of rule is commonly applied in groundwater management to promote long-term aquifer sustainability by restricting cumulative groundwater drawdown relative to the initial saturated thickness. Similar percentage-based limits are used in the Local Enhanced Management Area (LEMA) program in Kansas (Butler Jr et al., 2020). Such a rule provides a transparent, flexible, and easily implemented metric for balancing current water use with long-term aquifer health. In both study cases, groundwater storage remains sufficient over T = 20 years; so land values are unaffected by extraction rules.

In the HPA case, higher extraction rules increase water availability, extending operational years from 86 to 225 (Figure 10a1), with irrigation ceasing once the 8m limit is reached. Although longer operation times raise land values under T=TD, the gains are limited by discounting. CVaR and relative CVaR follow similar patterns.

In the SRB case, operational years range from 167 to 426 across extraction rules due to abundant water storage and relatively low use (Figure 10a2). The relative CVaR shows that the difference between expected land value and CVaR is less than 10%. This outcome is partly due to the long operational horizons and also suggests that variability in precipitation and prices has only a limited influence on economic results in this case.

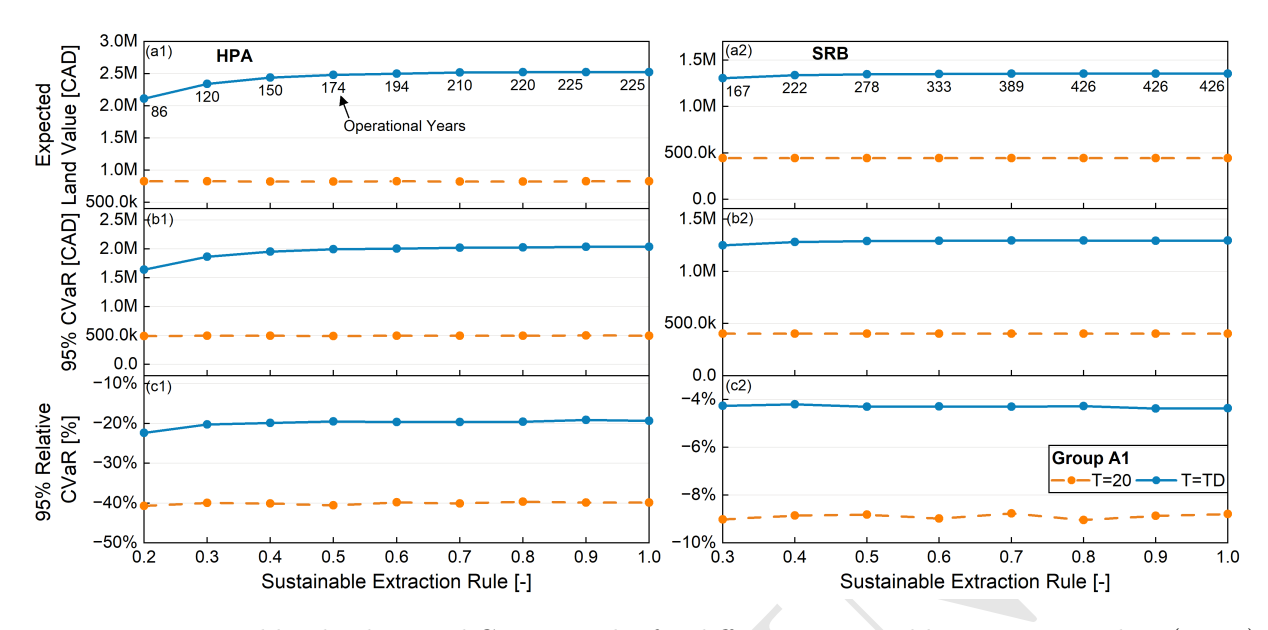


Figure 10: Expected land values and CVaR results for different sustainable extraction rules: (a1-c1) HPA farm site; (a2-c2) SRB farm site.

4.3 Climate Change

At the HPA site, projected declines in precipitation and rising temperatures reduce crop yields, thereby lowering land values (Figure 11a). Under RCP scenarios, land values are more negative at lower pumping limits compared to historic climate conditions. As the regulatory pumping limit relaxes, land values under historic conditions turn positive at a lower rate (2600 m³/day) than under the climate scenarios (3000 m³/day), indicating that more irrigation is needed to achieve optimal yields in more severe climates. When regulatory pumping is sufficient to meet crop water demand ($\bar{I} \geq 4000$ m³/day), differences in land values between historic and severe scenarios narrow to less than 12%. Severe climate conditions also result in lower CVaR values and greater variability in relative CVaR, especially for T=20 cases (Figure 11b, c). As pumping limits relax, both metrics stabilize and converge across scenarios.

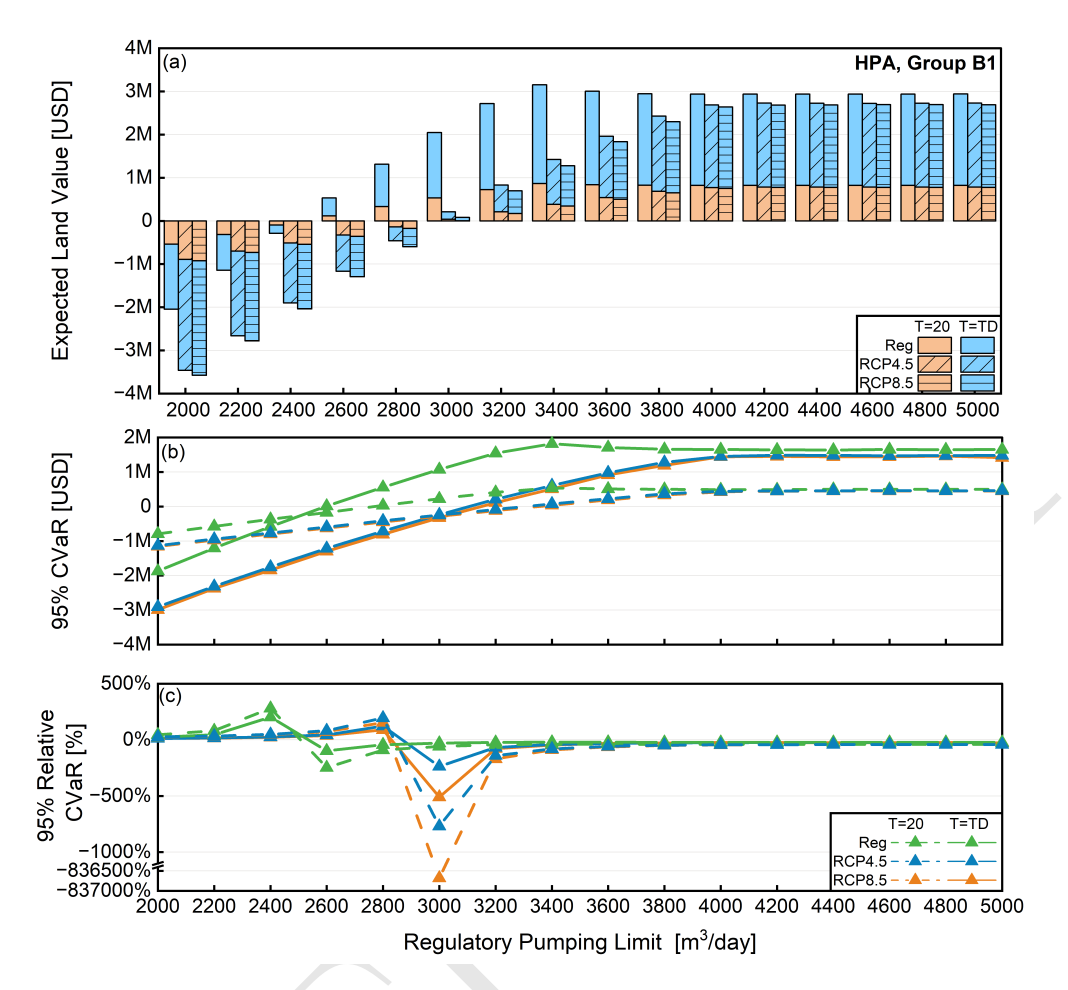


Figure 11: Climate change scenarios for the HPA site: (a) expected land values, (b) 95% CVaR and (c) relative CVaR.

The projected climate change scenarios are different in the SRB, as both precipitation and temperature are projected to increase, resulting in higher non-irrigated crop yields. In Figure 12, simulation results indicate that peak land values remain relatively unchanged and are reached with approximately the same regulatory pumping limit. All RCP scenarios yield slightly higher land values than baseline conditions (2%–4%) due to increased precipitation. CVaR and relative CVaR trends follow those of land values, with no significant bumps observed across scenarios (Figure 12b, c).

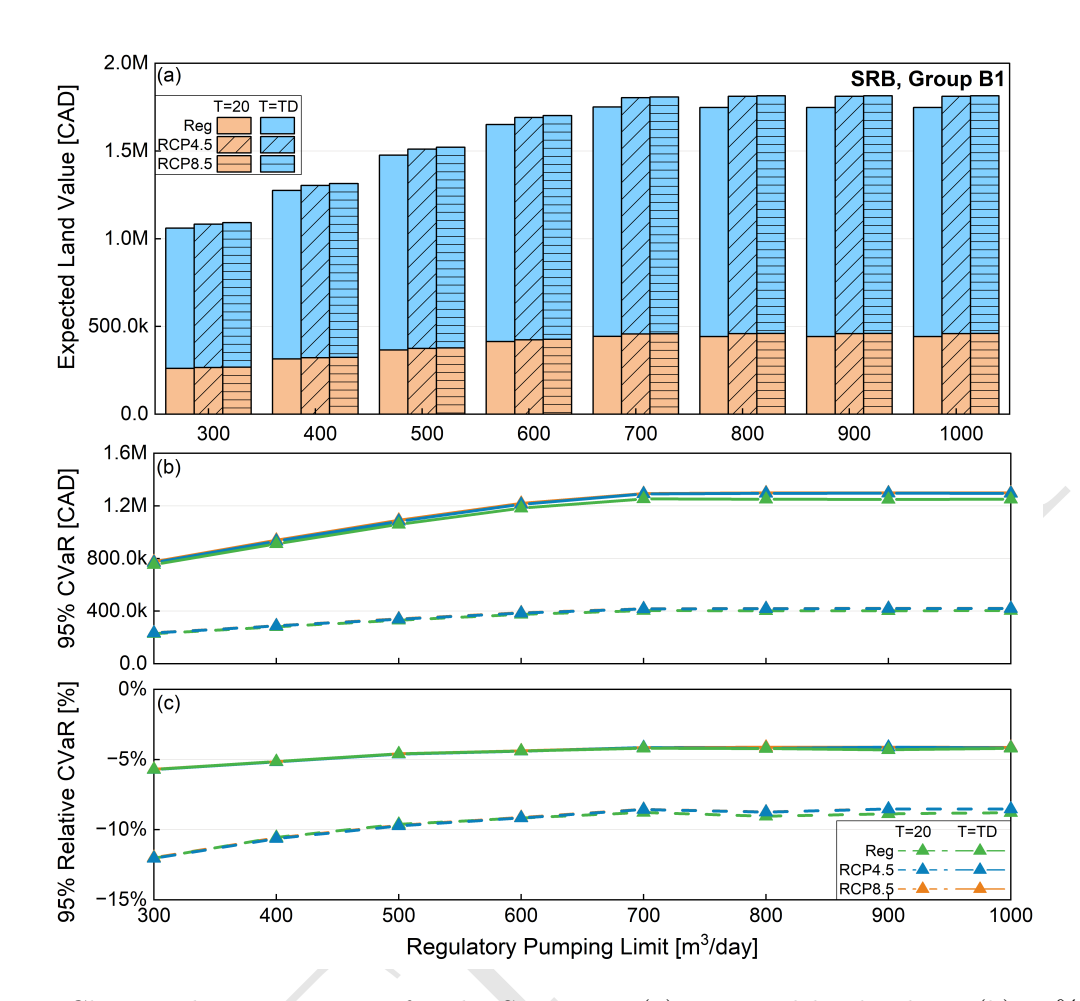


Figure 12: Climate change scenarios for the SRB site: (a) expected land values, (b) 95% CVaR and (c) relative CVaR.

5 Discussion

The discussion section addresses farmers' irrigation decisions, followed by regulatory constraints set by policymakers, and then outlines the study's limitations along with potential solutions.

5.1 Farmer's Decision

The farmer's decision is simulated using the irrigation fraction (β), representing the percentage of crop water demand to reach maximum yield each year. This decision strongly shaped outcomes. Larger irrigation fractions reduced operational years but generally increased land values, peaking around $\beta = 0.95 - 1$ (Figure 4). For both study sites, irrigation levels below 85% are not economically optimal for farmers. Two-stage strategies above $\beta = 0.9$ performed best, striking a balance between near-term gains and longer farm lifespans. These findings emphasize that farmer decisions must weigh both profitability and sustainability, particularly under changing environmental conditions.

5.2 Regulatory Constraints

In the HPA site (Figure 3), land value and CVaR peaked at regulatory pumping limit of ~3400 m³/day (below average demand of ~3700 m³/day), due to diminishing yield response, rising lift costs from greater drawdown, and reduced future availability. These results show that moderate regulatory pumping limits can outperform full irrigation by balancing short-term returns with long-term aquifer sustainability. In the SRB site (Figure 8), where irrigation combines groundwater and surface water, longer operational years muted these trends. Some scenarios extended >400 years, shifting the challenge from depletion to managing uncertainty over centuries. Sustainable extraction rules showed limited variation in outcomes (Figure 10), suggesting that simply allowing more water use does not guarantee higher returns, which is a key insight for setting regulatory constraints.

In HPA site, CVaR of annual cash flows was negative at early-stage pumping, indicating substantial downside risk can exist even when expected returns appear acceptable (Figure 6). Peak cash flows and steepest water depth derivatives occurred in years 6–7, marking this as a critical window for irrigation planning. Importantly, strategies with similar land values

often showed large differences in CVaR (Figure 5), highlighting that expected outcomes alone can be misleading. Incorporating CVaR is therefore essential to identify irrigation plans that minimize worst-case losses while maintaining long-term viability.

5.3 Climate Change

Preserving water for extended use can reduce future burdens, particularly under changing climates, where drier and hotter conditions in HPA site will raise irrigation requirements but lower land value compared to current scenarios. Peak land values for projected future climate scenarios for the HPA site occurred at ~4000 m³/day, and pumping above 3200 m³/day could avoid negative outcomes as indicated by CVaR results (Figure 11), but more water use accelerated depletion, raised energy costs, and can threaten ecosystems and downstream users. In contrast, in SRB site, climate change is projected to increase both precipitation and temperature, which slightly enhances land values in this region (Figure 12). However, this apparent benefit may be misleading, as the model does not account for extreme weather events that could reduce yields, raise operational costs, and introduce significant uncertainty.

5.4 Limitations

This study has several limitations. This study integrates surface water but neglects streamflow depletion, which may underestimate environmental impacts and future pumping costs. Climate change is represented only through precipitation and temperature, omitting factors such as extreme events and shifting growing seasons. Social and ecological consequences including land subsidence, ecosystem loss, and intergenerational costs are not modeled, and long-term discounting may understate the burden of depletion. Incorporating depletion penalties and broader climate and socioeconomic factors would provide a more realistic foundation for sustainable groundwater policy.

6 Conclusion

This research applies a farm-level hydro-economic model to two distinct sites, demonstrating how site-specific conditions influence irrigation performance and water-use outcomes. In simulations representing the hotter, drier, and more depleted HPA farm site, results indicate that the best-performing regulatory limit among the tested strategies is ~3400 m³/day, with the farmer's decision (i.e., irrigation fraction) around 0.95 under historical conditions. Under future climate scenarios, achieving comparable performance required a more relaxed regulatory limit for irrigation. For the SRB farm site, a relatively wetter and less depleted region, the best-performing regulatory limit is ~700 m³/day combined from groundwater and surface water, with groundwater providing the larger contribution and irrigation fractions in the range of 0.9–1 being preferred. Under future climate projections, no additional irrigation was needed due to increased precipitation. These findings highlight the importance of developing locally tailored water management strategies that reflect local hydrogeology, water availability, and climate patterns.

Beyond these cases, this study demonstrates the broader applicability of economic risk metrics in irrigation decision-making. CVaR is particularly useful in capturing downside risk that may be overlooked by average outcomes, showing that some strategies with positive land values can still expose farmers to severe losses. Integrating CVaR with climate projections offers a more robust framework for balancing short-term profitability with long-term ground-water sustainability. These insights can inform policies in other agricultural regions facing similar trade-offs between water scarcity, climate variability, and economic viability.

7 Author Contributions

B.T.: Conceptualization, Methodology, Data curation, Software, Validation, Visualization, Writing – original draft, Writing – review and editing. A.B.: Conceptualization, Methodology, Validation, Supervision, Writing – review and editing, Project administration, Funding acquisition. M.I.: Methodology, Validation, Writing – review and editing. D.R.: Writing – review and editing.

8 Funding Sources

This work was supported by a University of Waterloo Water Institute Seed Grant; University of Waterloo Trailblazer Award; and the Natural Sciences and Engineering Research Council of Canada [Discovery Grant].

References

- AFCC (2013), 'AAFC Watershed Project', https://open.canada.ca/data/en/dataset/c20d97e7-60d8-4df8-8611-4d499a796493. Accessed: 2024-10-01.
- AFSC (2023), 'Yield Alberta-2023', https://afsc.ca/wp-content/uploads/2023/02/ Yield-Alberta-2023.pdf. Accessed: 2024-10-01.
- Ajaz, A., Datta, S. and Stoodley, S. (2020), 'High plains aquifer—state of affairs of irrigated agriculture and role of irrigation in the sustainability paradigm', Sustainability 12(9), 3714.
- Alam, M. F., Pavelic, P., Sikka, A., Krishnan, S., Dodiya, M., Bhadaliya, P. and Joshi, V. (2023), 'Energy consumption as a proxy to estimate groundwater abstraction in irrigation', Groundwater for Sustainable Development 23, 101035.
- Alberta Climate Information Service (2024), 'ACIS Find historic climate data', https://acis.alberta.ca/acis/weather-data-viewer.jsp. Accessed: 2024-10-01.
- Allen, R. G., Pereira, L. S., Raes, D., Smith, M. et al. (1998), 'Crop evapotranspiration-guidelines for computing crop water requirements-fao irrigation and drainage paper 56', Fao, Rome 300(9), D05109.
- An, Y., Liang, J., Schild, S. E., Bues, M. and Liu, W. (2017), 'Robust treatment planning with conditional value at risk chance constraints in intensity-modulated proton therapy', *Medical physics* **44**(1), 28–36.
- Bates, B., Kundzewicz, Z. and Wu, S. (2008), *Climate change and water*, Intergovernmental Panel on Climate Change Secretariat.
- Brookfield, A. (2016), 'Minimum saturated thickness calculator', Kansas Geological Survey Open-File Report 3.
- Bruneau, J. (2009), 'Human activities and water use in the south saskatchewan river basin joel bruneau, darrell r. corkal, elise pietroniro, brenda toth, and garth van der kamp', A dry oasis: Institutional adaptation to climate on the Canadian Plains 24, 129.
- Butler Jr, J., Bohling, G., Whittemore, D. and Wilson, B. (2020), 'Charting pathways toward sustainability for aquifers supporting irrigated agriculture', *Water Resources Research* **56**(10), e2020WR027961.
- Cederstrand, J. R. and Becker, M. F. (1998), Digital map of hydraulic conductivity for the high plains aquifer in parts of colorado, kansas, nebraska, new mexico, oklahoma, south dakota, texas, and wyoming, Technical report.
- Chen, J., Famigliett, J. S., Scanlon, B. R. and Rodell, M. (2016), 'Groundwater storage changes: present status from grace observations', *Remote sensing and water resources* pp. 207–227.

- Climate Data (2024), 'Climate Data: Vulcan County', https://climatedata.ca/. Accessed: 2024-10-01.
- Cooper Jr, H. and Jacob, C. E. (1946), 'A generalized graphical method for evaluating formation constants and summarizing well-field history', *Eos, Transactions American Geophysical Union* **27**(4), 526–534.
- Corkal, D. R., Diaz, H. and Sauchyn, D. (2011), 'Changing roles in canadian water management: a case study of agriculture and water in canada's south saskatchewan river basin', *International Journal of Water Resources Development* **27**(4), 647–664.
- Cotterman, K. A., Kendall, A. D., Basso, B. and Hyndman, D. W. (2018), 'Groundwater depletion and climate change: future prospects of crop production in the central high plains aquifer', *Climatic change* **146**, 187–200.
- Cummings, D. I., Russell, H. A. and Sharpe, D. R. (2012), 'Buried-valley aquifers in the canadian prairies: geology, hydrogeology, and origin', *Canadian Journal of Earth Sciences* **49**(9), 987–1004.
- Edwards, E. C. (2016), 'What lies beneath? aquifer heterogeneity and the economics of groundwater management', *Journal of the Association of Environmental and Resource Economists* 3(2), 453–491.
- Esteve, P., Varela-Ortega, C., Blanco-Gutiérrez, I. and Downing, T. E. (2015), 'A hydroeconomic model for the assessment of climate change impacts and adaptation in irrigated agriculture', *Ecological Economics* **120**, 49–58.
- Faghih-Roohi, S., Ong, Y.-S., Asian, S. and Zhang, A. N. (2016), 'Dynamic conditional value-at-risk model for routing and scheduling of hazardous material transportation networks', *Annals of Operations Research* **247**, 715–734.
- Filippi, C., Guastaroba, G. and Speranza, M. G. (2020), 'Conditional value-at-risk beyond finance: a survey', *International Transactions in Operational Research* **27**(3), 1277–1319.
- Foster, S., Hirata, R., Vidal, A., Schmidt, G. and Garduño, H. (2009), 'The guarani aquifer initiative—towards realistic groundwater management in a transboundary context', *World Bank*.
- Fowler, A. and Hennessy, K. (1995), 'Potential impacts of global warming on the frequency and magnitude of heavy precipitation', *Natural Hazards* 11, 283–303.
- GIN (2021), 'Groundwater Information Network: Buried Valleys Aquifer System', https://gin.gw-info.net/service/api_ngwds:gin2/en/data/standard.hydrogeologicunit.html?id=216. Accessed: 2024-10-01.
- Gober, P. and Wheater, H. (2014), 'Socio-hydrology and the science-policy interface: a case study of the saskatchewan river basin', *Hydrology and Earth System Sciences* **18**(4), 1413–1422.

- Government of Alberta (2020), 'Alberta Water Well Information Database (or Baseline Water Well Test Database)', http://groundwater.alberta.ca/WaterWells/d/. Accessed: 2024-10-01.
- Government of Alberta (2023), 'Environment and Protected Areas', https://avw.alberta.ca/ApprovalViewer.aspx. Accessed: 2024-10-01.
- Government of Alberta (2024a), 'Cost and return benchmarks for crops and forages: irrigated crops', https://afsc.ca/wp-content/uploads/2023/02/Yield-Alberta-2023.pdf. Accessed: 2024-10-01.
- Government of Alberta (2024b), 'Cropland by municipality', https://open.canada.ca/data/en/dataset/6e883463_f7e6_4e48_9909_67182e0e4dbc. Accessed: 2024-10-01.
- Government of Alberta (2024c), 'Guide to Groundwater Authorization'. Accessed: 2025-02-19.
 - $\textbf{URL:} \ https://open.alberta.ca/publications/guide_to_groundwater_authorization_summary$
- Griebler, C. and Avramov, M. (2015), 'Groundwater ecosystem services: a review', Freshwater Science 34(1), 355–367.
- Harou, J. J., Pulido-Velazquez, M., Rosenberg, D. E., Medellín-Azuara, J., Lund, J. R. and Howitt, R. E. (2009), 'Hydro-economic models: Concepts, design, applications, and future prospects', *Journal of Hydrology* **375**(3-4), 627–643.
- Hemathilake, D. and Gunathilake, D. (2022), Agricultural productivity and food supply to meet increased demands, in 'Future foods', Elsevier, pp. 539–553.
- High Plains Regional Climate Center (2024), 'High Plains Regional Climate Center: Monthly Precipitation', http://climod.unl.edu/. Accessed: 2024-10-01.
- Hund, S. V., Allen, D. M., Morillas, L. and Johnson, M. S. (2018), 'Groundwater recharge indicator as tool for decision makers to increase socio-hydrological resilience to seasonal drought', *Journal of Hydrology* **563**, 1119–1134.
- Ibendahl, G., O'Brien, D., Lancaster, S., Holman, J. and Haag, L. (2023), 'Corn cost-return budget (w-c-f rotation) in southwest kansas', https://agmanager.info/farm-budgets/2024-farm-management-guides-irrigated-crops. Accessed: 2024-08-22.
- Insley, M. C. and Wirjanto, T. S. (2010), 'Contrasting two approaches in real options valuation: contingent claims versus dynamic programming', *Journal of Forest Economics* **16**(2), 157–176.
- Islam, S. M. F. and Karim, Z. (2019), 'World's demand for food and water: The consequences of climate change', *Desalination-challenges and opportunities* **2019**.

- Ji, L. and Senay, G. B. (2023), 'Temporal trends in agricultural water use and the relationships to hydroclimatic factors in the high plains aquifer region', JAWRA Journal of the American Water Resources Association 59(5), 950–969.
- Kansas Water Appropriation Act (2022), 'Kansas water appropriation act', https://www.agriculture.ks.gov/home/showpublisheddocument/1812/638457552336500000. Retrieved from Kansas Department of Agriculture.
- KGS (2025), 'Water Information Management and Analysis System (WIMAS)', https://geohydro.kgs.ku.edu/geohydro/wimas/query_setup.cfm. Accessed: 2024-10-01.
- Klocke, N. L. (2011), 'Development of crop production functions for irrigation in north central kansas'.
- Lambert, F. H., Stine, A. R., Krakauer, N. Y. and Chiang, J. C. (2008), 'How much will precipitation increase with global warming?', EOS, Transactions American Geophysical Union 89(21), 193–194.
- Lin, C.-Y., Alegria, M. E. O., Dhakal, S., Zipper, S. and Marston, L. (2024), 'Pychamp: A crop-hydrological-agent modeling platform for groundwater management', *Environmental Modelling & Software* 181, 106187.
- Ma, Q., Yang, Y., Sheng, Z., Han, S., Yang, Y. and Moiwo, J. P. (2022), 'Hydro-economic model framework for achieving groundwater, food, and economy trade-offs by optimizing crop patterns', *Water Research* **226**, 119199.
- Martin, D. L., Supalla, R. J., Thompson, C. L., McMullen, B. P., Hergert, G. W. and Burgener, P. A. (2010), Advances in deficit irrigation management, *in* '5th National Decennial Irrigation Conference Proceedings, 5-8 December 2010, Phoenix Convention Center, Phoenix, Arizona USA', American Society of Agricultural and Biological Engineers, p. 1.
- Masud, M., Khaliq, M. and Wheater, H. (2015), 'Analysis of meteorological droughts for the saskatchewan river basin using univariate and bivariate approaches', *Journal of Hydrology* **522**, 452–466.
- Mieno, T., Foster, T., Kakimoto, S. and Brozović, N. (2024), 'Aquifer depletion exacerbates agricultural drought losses in the us high plains', *Nature Water* **2**(1), 41–51.
- Mishra, R. K. (2023), 'Fresh water availability and its global challenge', British Journal of Multidisciplinary and Advanced Studies 4(3), 1–78.
- Misra, A. K. (2014), 'Climate change and challenges of water and food security', *International Journal of Sustainable Built Environment* **3**(1), 153–165.
- Ortiz-Bobea, A., Ault, T. R., Carrillo, C. M., Chambers, R. G. and Lobell, D. B. (2021), 'Anthropogenic climate change has slowed global agricultural productivity growth', *Nature Climate Change* **11**(4), 306–312.

- Ortiz-Partida, J. P., Fernandez-Bou, A. S., Maskey, M., Rodríguez-Flores, J. M., Medellín-Azuara, J., Sandoval-Solis, S., Ermolieva, T., Kanavas, Z., Sahu, R. K., Wada, Y. et al. (2023), 'Hydro-economic modeling of water resources management challenges: Current applications and future directions', *Water Economics and Policy* 9(01), e2340003.
- Peck, J. C. (2015), 'Legal challenges in government imposition of water conservation: The kansas example', *Agronomy Journal* **107**(4), 1561–1566.
- Pomeroy, J., de Boer, D. and Martz, L. W. (2005), Hydrology and water resources of saskatchewan, Technical report, Centre for Hydrology, University Saskatchewan, Saskatchewan, Saskatchewan.
- Qi, S. (2010), Digital map of the aquifer boundary for the high plains aquifer in parts of colorado, kansas, nebraska, new mexico, oklahoma, south dakota, texas, and wyoming, Technical report, US Geological Survey.
- Rajan, N., Maas, S., Kellison, R., Dollar, M., Cui, S., Sharma, S. and Attia, A. (2015), 'Emitter uniformity and application efficiency for centre-pivot irrigation systems', *Irrigation and Drainage* **64**(3), 353–361.
- Richardson, C. W. (1981), 'Stochastic simulation of daily precipitation, temperature, and solar radiation', *Water resources research* 17(1), 182–190.
- Rockafellar, R. T. and Uryasev, S. (2002), 'Conditional value-at-risk for general loss distributions', *Journal of banking & finance* **26**(7), 1443–1471.
- Rockafellar, R. T., Uryasev, S. et al. (2000), 'Optimization of conditional value-at-risk', Journal of risk 2, 21–42.
- Rohde, M. M., Froend, R. and Howard, J. (2017), 'A global synthesis of managing groundwater dependent ecosystems under sustainable groundwater policy', *Groundwater* **55**(3), 293–301.
- Sahoo, S., Russo, T., Elliott, J. and Foster, I. (2017), 'Machine learning algorithms for modeling groundwater level changes in agricultural regions of the us', *Water Resources Research* **53**(5), 3878–3895.
- Scanlon, B. R., Fakhreddine, S., Rateb, A., de Graaf, I., Famiglietti, J., Gleeson, T., Grafton, R. Q., Jobbagy, E., Kebede, S., Kolusu, S. R. et al. (2023), 'Global water resources and the role of groundwater in a resilient water future', *Nature Reviews Earth & Environment* 4(2), 87–101.
- Scanlon, B. R., Faunt, C. C., Longuevergne, L., Reedy, R. C., Alley, W. M., McGuire, V. L. and McMahon, P. B. (2012), 'Groundwater depletion and sustainability of irrigation in the us high plains and central valley', *Proceedings of the national academy of sciences* 109(24), 9320–9325.

- Smidt, S. J., Haacker, E. M., Kendall, A. D., Deines, J. M., Pei, L., Cotterman, K. A., Li, H., Liu, X., Basso, B. and Hyndman, D. W. (2016), 'Complex water management in modern agriculture: Trends in the water-energy-food nexus over the high plains aquifer', Science of the Total Environment 566, 988–1001.
- Stanton, J. (2013), 'Ds-777 average annual recharge, 2000 to 2009, in inches estimated from the soil water balance (swb) model for the high plains aquifer in parts of colorado, kansas, nebraska, new mexico, oklahoma, south dakota, texas, and wyoming: U.s. geological survey data release'.
- Statistics Canada (2024), 'Table 32-10-0077-01 Farm product prices, crops and livestock'. Accessed: 2024-10-01.
- Steward, D. R., Bruss, P. J., Yang, X., Staggenborg, S. A., Welch, S. M. and Apley, M. D. (2013), 'Tapping unsustainable groundwater stores for agricultural production in the high plains aquifer of kansas, projections to 2110', *Proceedings of the National Academy of Sciences* **110**(37), E3477–E3486.
- Taylor, R. G., Scanlon, B., Döll, P., Rodell, M., Van Beek, R., Wada, Y., Longuevergne, L., Leblanc, M., Famiglietti, J. S., Edmunds, M. et al. (2013), 'Ground water and climate change', *Nature climate change* 3(4), 322–329.
- The Climate Explorer (2024), 'U.S. Climate Resilience Toolkit CLIMATE EXPLORER: Haskell County', https://crt-climate-explorer.nemac.org/. Accessed: 2024-10-01.
- Tian, B., Brookfield, A. and Insley, M. (2025), 'Development of a coupled hydro-economic model to support groundwater irrigation decisions', *EarthArXiv*. Preprint.
- U.S. Bureau of Labor Statistic (2024), 'Consumer Price Index', https://www.bls.gov/cpi/. Accessed: 2024-10-01.
- U.S. Energy Information Administration (2024), 'Average price of electricity to ultimate customers by end-use sector', https://www.eia.gov/electricity/monthly. Accessed: 2024-10-01.
- USDA (2017), 'Total and Per Farm Overview, 2017 and change since 2012: Haskell County Kansas', https://www.nass.usda.gov/Publications/AgCensus/2017/Online_Resources/County_Profiles/Kansas/cp20081.pdf. Accessed: 2024-10-01.
- USDA (2024), 'Prices Received: Corn Prices Received by Month, US', https://www.nass.usda.gov/Charts_and_Maps/Agricultural_Prices/pricecn.php. Accessed: 2024-10-01.
- USGS (2023a), 'Saturated thickness, High Plains aquifer, 2009 [Data set]. U.S. Geological Survey', https://doi.org/10.5066/P9WMRZBN. Accessed: 2024-10-01.
- USGS (2023b), 'Specific yield, High Plains aquifer [Data set]. U.S. Geological Survey', https://doi.org/10.5066/P9XWB5JH. Accessed: 2024-10-01.

- Van Vuuren, D. P., Edmonds, J., Kainuma, M., Riahi, K., Thomson, A., Hibbard, K., Hurtt, G. C., Kram, T., Krey, V., Lamarque, J.-F. et al. (2011), 'The representative concentration pathways: an overview', *Climatic change* **109**, 5–31.
- White, J. W., Hoogenboom, G., Kimball, B. A. and Wall, G. W. (2011), 'Methodologies for simulating impacts of climate change on crop production', *Field Crops Research* **124**(3), 357–368.
- Xu, X., Meng, Z. and Shen, R. (2013), 'A tri-level programming model based on conditional value-at-risk for three-stage supply chain management', *Computers & Industrial Engineering* **66**(2), 470–475.
- Xuan, A., Shen, X., Guo, Q. and Sun, H. (2021), 'A conditional value-at-risk based planning model for integrated energy system with energy storage and renewables', *Applied Energy* **294**, 116971.
- Yang, G., Li, S., Wang, H. and Wang, L. (2022), 'Study on agricultural cultivation development layout based on the matching characteristic of water and land resources in north china plain', *Agricultural Water Management* **259**, 107272.
- Yang, X. (2022), An analysis of optimal agricultural fertilizer application decisions in the presence of market and weather uncertainties and nutrient pollution, PhD thesis, University of Waterloo.
- Yao, Y., Lund, J. R. and Medellín-Azuara, J. (2024), 'Combining crop and water decisions to manage groundwater overdraft over decadal and longer timescales', *Water* **16**(9), 1223.
- Zhang, X., Hao, Z., Singh, V. P., Zhang, Y., Feng, S., Xu, Y. and Hao, F. (2022), 'Drought propagation under global warming: Characteristics, approaches, processes, and controlling factors', *Science of the Total Environment* 838, 156021.

A Parameters

Table A1: Model parameters for HPA and SRB sites

Parameter	Description (Unit)	Value		Source		
		HPA SRB		НРА	SRB	
_	Growing season	Apr-Sept	May-Aug	-	-	
-	Non-growing season	Oct-Mar	Sept-Apr	-	_	
λ_g	Distribution parameter for growing season (-)	0.017	0.0163	CAL^a	CAL	
λ_{ng}	Distribution parameter for non-growing season (-)	0.0477	0.0525	CAL	CAL	
ET_r	Reference evapotranspiration (m/yr)	1.182	0.649	CAL	CAL	
K_c	Daily crop coefficient, corn/barley (-)	0.58	0.65	Allen et al. (1998)	Allen et al. (1998)	
Y_m	Maximum potential yield (bushel per acre)	225	126	Ibendahl et al. (2023)	AFSC (2023)	
I_e	Irrigation efficiency, center pivot irrigation system (-)	0.9	0.9	Rajan et al. (2015)	Rajan et al. (2015)	
P_e	Precipitation efficiency (-)	0.8	0.8	AE^b	AE	
r_w	Effective radius of the well (m)	0.2032	0.07	KGS (2025)	Government of Alberta (2023)	
t_p	Duration of pumping (day)	183	123	_	_	
t_s	Time since the start of pumping (day)	365	365	_	_	
t_c	Time since the start of cessation (day)	182	242	-	_	
w_{eff}	Well efficiency (-)	0.8	0.8	AE	AE	
Y_n	Non-irrigated yield (bu/acre)	82	75	Ibendahl et al. (2023)	AFSC (2023)	
b_{slope}	Slope of yield-evapotranspiration function (bu/ac/inch)	11.2	6	Klocke (2011)	Klocke (2011)	
b_{cc}	Yield factor (-)	0.46	0.79	AE	AE	
c(1)	OLS parameter (-)	-0.04114	-0.06673	CAL	CAL	
c(2)	OLS parameter (-)	0.2049	0.4492	CAL	CAL	
θ	Speed of mean reversion (-)	0.4937	0.8008	CAL	CAL	
se_m	OLS parameter (-)	0.05168	0.05719	CAL	CAL	
σ_m	Volatility (-)	0.179	0.1981	CAL	CAL	

Continued on next page

Table A1 – Continued from previous page $\,$

Parameter	Description (Unit)	Value		Source		
		НРА	SRB	НРА	SRB	
\bar{P}	Long-run mean (2024 USD/CAD	4.982	6.7315	USDA (2024)	Statistics Canada	
	per bushel)				(2024)	
ho	Water density (kg/m^3)	1000	1000	_	_	
g	Gravity factor (m/s^2)	9.81	9.81	-	-	
η_p	Pumping efficiency (-)	0.8	0.8	AE	AE	
C_y	Fertilizer cost (USD/CAD per bu)	0.71	1.03	Ibendahl et al. (2023)	Government of Alberta	
					(2024a)	
C_f	Fixed cost (USD/CAD per acre)	820.35	366.11	Ibendahl et al. (2023)	Government of Alberta	
					(2024a)	
C_e	Electricity Price (USD/CAD per	0.12	0.135	U.S. Energy Informa-	Government of Alberta	
	kWh)			tion Administration	(2024a)	
				(2024)		
Area	Farm size (acre)	371	89	KGS (2025)	Government of Alberta	
					(2023)	
H_0	Static water level (m)	108.2	26.5	KGS (2025)	Government of Alberta	
					(2023)	

^a Calculated results (CAL).

 $^{^{\}rm b}$ Authors' elaboration (AE).

B Price Model

We conducted 10,000 Monte Carlo simulations of the price models and validated them using Maximum Likelihood Estimation (MLE) (Yang, 2022). Model fit and Monte Carlo results for the HPA site are presented in Tian et al. (2025). For the SRB site, the standard errors of the parameters estimated using the MLE are $se_{\theta} = 0.4013$, $se_{\bar{P}} = 0.5481$, and $se_{\sigma} = 0.0131$.

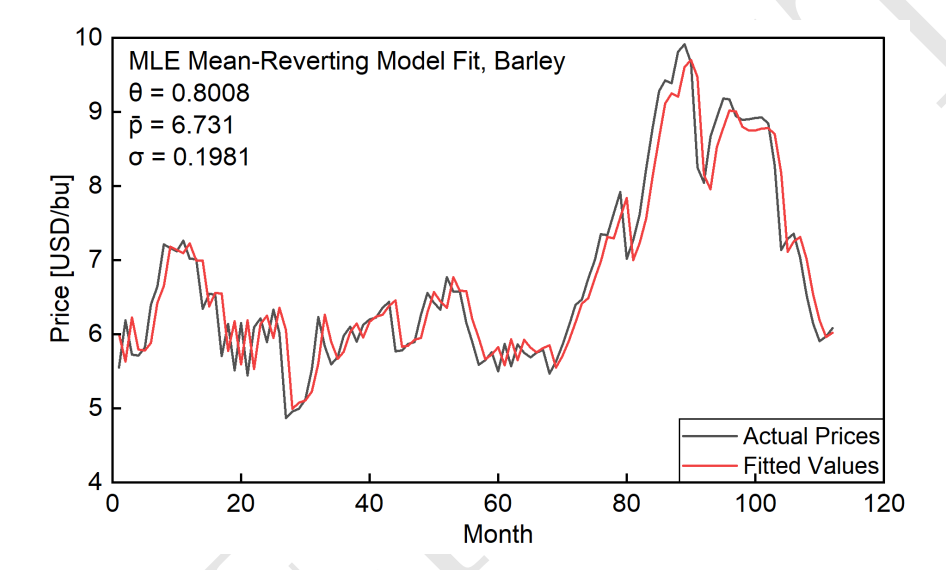


Figure B-1: MLE simulated data and historical prices, SRB.

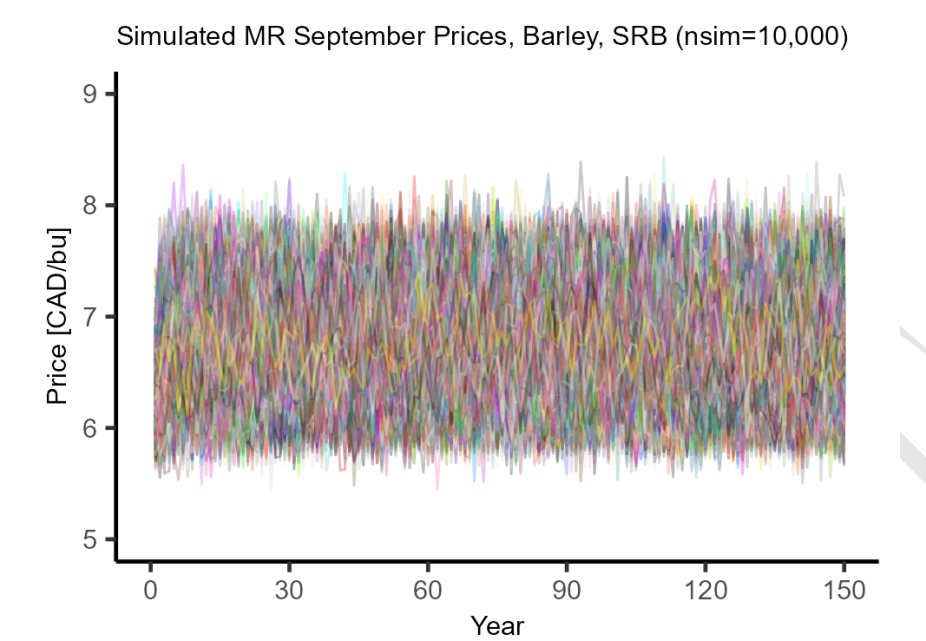


Figure B-2: Price estimations of 10,000 times Monte Carlo simulation for SRB.

C Annual Cash Flow Analysis of the SRB site

In Figure C-1, expected annual cash flows in the SRB site follow a similar pattern to the HPA site, peaking around years 3–5. Beyond a regulatory pumping limit of 700 m³/day, simulated outcomes are almost same, and have minimal variation. For the T=TD case, annual cash flows approach zero after ~200 years due to discounting, complicating long-term planning by requiring consideration of both discounted economic returns and water sustainability.

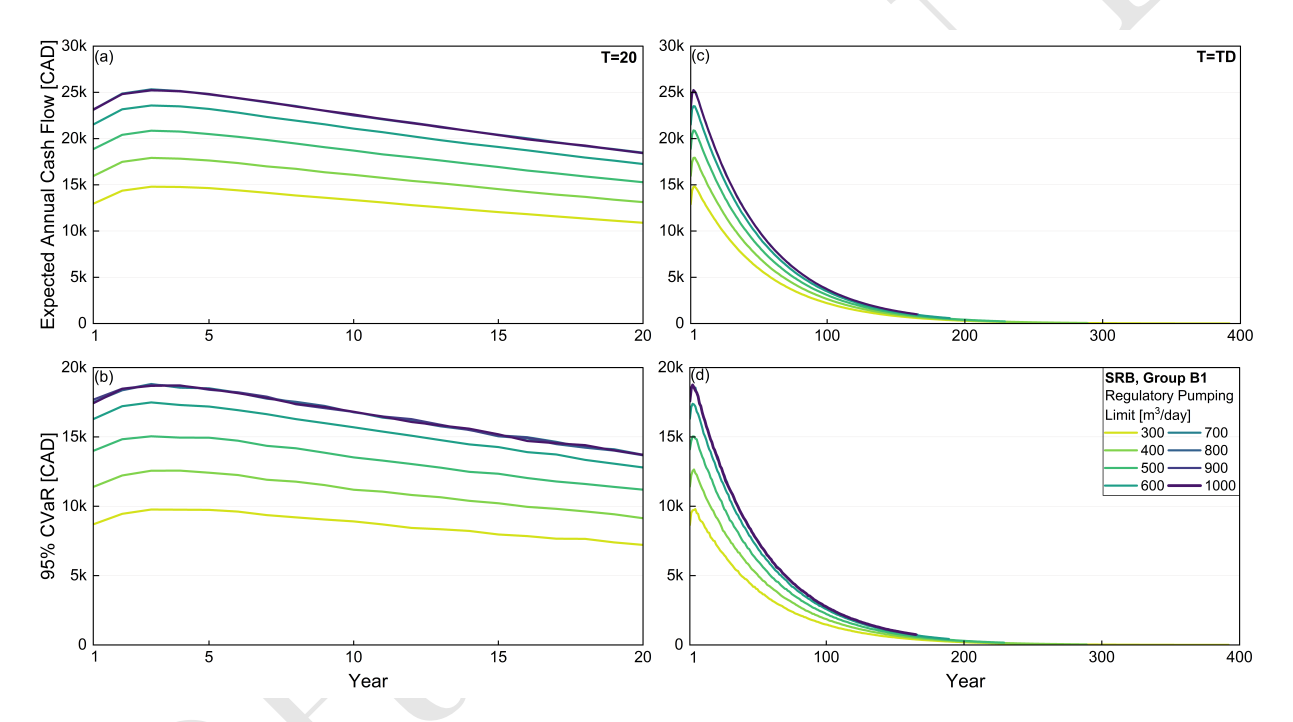


Figure C-1: (a, c) Expected annual cash flow; (b, d) corresponding CVaR of strategy group B1 in the SRB site.